A Manganese(III) Complex of 3,5-Bis((salicylideneamino)methyl)pyrazole: Synthesis, Structure, and Properties

Kenji Shindo, Yumika Mori, Ken-ichiro Motoda, Hiroshi Sakiyama, Naohide Matsumoto, and Hisashi Ōkawa*

Department of Chemistry, Faculty of Science, Kyushu University, Hakozaki 6-10-1, Higashiku, Fukuoka 812, Japan

Received April 6, 1992

3,5-Bis((salicylideneamino)methyl)pyrazole forms a manganese(III) complex of the formula $Mn_4(L)_2(CH_3O)_4(CH_3OH)_8(ClO_4)_2$ that crystallizes in the triclinic crystal system, space group $P\bar{1}$, with $Z = 1$, $a = 13.663$ (6) Å, $b = 14.536$ (4) Å, $c = 8.483$ (4) Å, $\alpha = 98.59$ (4)°, $\beta = 103.98$ (5)°, $\gamma = 92.77$ (6)°, and $V = 1611$ (1) Å^3. The refinement converged with $R = 0.0768$ and $R_w = 0.0734$ based on 4525 reflections with $|F_o| > 3\sigma(|F_o|)$. The crystal structure analysis reveals the presence of the centrosymmetric complex cation $[Mn_4(L)_2(CH_3O)_4(CH_3OH)_4]^{2+}$ with four linearly arrayed Mn(III) ions. Each terminal Mn(III) ion is bound at one NNO-coordination site of L^{3-}, through a pyrazolate nitrogen and salicylideneaminate nitrogen and oxygen, and assumes a distorted octahedral geometry together with two methanol oxygens and one methoxide oxygen acting as a bridge to the adjacent internal Mn(III) ion. The pyrazolate nitrogen of the other NNO site coordinates to the adjacent internal Mn(III) ion, but the salicylideneaminate nitrogen and oxygen are associated with coordination to another internal Mn(III) ion. The separation between the terminal and internal Mn(III) ions, bridged by the pyrazolate group and methoxide ion, is 3.485 (3) Å. The two internal Mn(III) ions are bridged to each other by two methoxide oxygens (Mn- -Mn = 3.127 (2) Å), and each metal assumes a distorted octahedral configuration. Cryomagnetic investigations in the temperature range 4.2–300 K on solid samples demonstrate weak antiferromagnetic spin-exchange within each molecule. In *N,N*-dimethylformamide the complex assumes a dinuclear structure with two Mn(III) ions at the two NNO-coordination sites and shows a high catalase-like activity.

Introduction

Recently, oligonuclear manganese complexes have received significant attention[1,2] because of the involvement of such species in biological systems, for example Mn catalase,[3,4] Mn ribonucleotide reductase,[5] and the oxygen-evolving center (OEC) of photosystem II (PSII) in green plants and algae.[6] On the basis of a variety of studies, it is now known that two manganese ions are involved in Mn catalase and Mn ribonucleotide reductase and four manganese ions are involved in the OEC of PSII. The X-ray structure analysis for *Thermus thermophilus* Mn catalase indicates the Mn–Mn separation of 3.6 Å,[7] and model studies have suggested that the inner-sphere interaction of H_2O_2 with the dinuclear manganese center is the key step in catalase activity.[8,9] There have been obtained some dinuclear manganese complexes that exhibit catalase-like activity,[8-12] and the first example of a peroxo-bridged dinuclear manganese complex was reported by Wieghardt and co-workers very recently.[13] With the hope of mimicking the physical and structural characteristics of the OEC of PSII, tetranuclear Mn complexes of "adamantane",[14] "butterfly",[15-17] "cubane",[18-20] and "dimer of dimer"[21-23] types were obtained, but functional modelings of the OEC are very few.[24] A possible mechanistic scheme of the OEC is proposed involving the oxidative conversion of two coordinated OH^- or H_2O groups to a bridging O_2^{2-} group prior to the evolution of O_2.[6,25] Recently it was found that the OEC of PSII (S_2 state)

(1) Wieghardt, K. *Angew. Chem., Int. Ed. Engl.* **1989**, *28*, 1153.
(2) Christou, G. *Acc. Chem. Res.* **1989**, *22*, 328.
(3) (a) Khangulov, S. V.; Barynin, V. V.; Melik-Adamyan, U. R.; Grebenko, A. I.; Voevedskaya, N. V.; Blumenfeld, L. A.; Dobryakov, S. N.; Ilyasova, V. B. *Bioorg. Khim.* **1986**, *12*, 741. (b) Fronko, R. M.; Penner-Harn, J. E.; Bender, C. J. *J. Am. Chem. Soc.* **1988**, *110*, 7554.
(4) Allgood, G. S.; Perry, J. J. *J. Bacteriol.* **1986**, *168*, 563.
(5) (a) Wariishi, H.; Akileswaran, L.; Gold, M. H. *Biochemistry* **1988**, *27*, 5365. (b) Glenn, J. K.; Akileswaran, L.; Gold, M. H. *Arch. Biochem. Biophys.* **1986**, *251*, 688.
(6) (a) Brudvig, G. W.; Crabtree, R. H. *Proc. Natl. Acad. Sci. U.S.A.* **1986**, *83*, 4586. (b) Dismukes, G. C. *Photochem. Photobiol.* **1986**, *43*, 99. (c) Beck, W. F.; Brudvig, G. W. *J. Am. Chem. Soc.* **1988**, *110*, 1517. (d) Brudvig, G. W.; Beck, W. F. *Annu. Rev. Biophys. Biophys. Chem.* **1989**, *18*, 25 and references therein.
(7) Barynin, V. V.; Vagin, A. A.; Melik-Adamyan, V. R.; Grebenko, A. I.; Khangulov, S. V.; Popov, A. N.; Andrianova, M. E.; Vainshtein, B. K. *Sov. Phys. Dokl.* **1986**, *31*, 457.
(8) Oishi, N.; Nishida, Y.; Kida, S. *Chem. Lett.* **1982**, 409.
(9) (a) Larson, E. J.; Pecoraro, V. L. *J. Am. Chem. Soc.* **1991**, *113*, 3810. (b) Larson, E. J.; Pecoraro, V. L. *J. Am. Chem. Soc.* **1991**, *113*, 7809. (c) Larson, E. J.; Riggs, P. J.; Penner-Hahn, J. E.; Pecoraro, V. L. *J. Chem. Soc., Chem. Commun.* **1992**, 102.
(10) Nishida, Y.; Nasu, M. *Inorg. Chim. Acta* **1991**, *190*, 1.
(11) Mathur, P.; Crowder, M.; Dismukes, G. C. *J. Am. Chem. Soc.* **1987**, *109*, 5227.
(12) Naruta, Y.; Maruyama, K. *J. Am. Chem. Soc.* **1991**, *113*, 3595.
(13) Bossek, U.; Weyhermuller, T.; Wieghardt, K.; Nuber, B.; Weiss, J. *J. Am. Chem. Soc.* **1990**, *112*, 6387.
(14) (a) Wieghardt, K.; Bossek, U.; Nuber, B.; Weiss, J.; Bonvoisin, J.; Corbella, M.; Vitols, S. E.; Girerd, J.-J. *J. Am. Chem. Soc.* **1988**, *110*, 7398. (b) Wieghardt, K.; Bossek, U.; Gebert, W. *Angew. Chem., Int. Ed. Engl.* **1983**, *22*, 328.
(15) Vincent, J. B.; Christmas, C.; Huffman, J. C.; Christou, G.; Chang, H.-R.; Hendrickson, D. N. *J. Chem. Soc., Chem. Commun.* **1987**, 236.
(16) Christmas, C.; Vincent, J. B.; Huffman, J. C.; Christou, G.; Chang, H.-R.; Hendrickson, D. N. *J. Chem. Soc., Chem. Commun.* **1987**, 1303.
(17) Kulawiec, R. J.; Crabtree, R. H.; Brudvig, G. W.; Schulte, G. K. *Inorg. Chem.* **1988**, *27*, 1311.
(18) McKee, V.; Shepard, W. B. *J. Chem. Soc., Chem. Commun.* **1985**, 158.
(19) Li, Q.; Vincent, J. B.; Libby, E.; Chang, H.-R.; Huffman, J. C.; Boyd, P. D. W.; Christou, G.; Hendrickson, D. N. *Angew. Chem., Int. Ed. Engl.* **1988**, *27*, 1731.
(20) Bashkin, J. S.; Chang, H.-R.; Streib, W. E.; Huffman, J. C.; Hendrickson, D. N.; Christou, G. *J. Am. Chem. Soc.* **1987**, *109*, 6502.
(21) Chan, M. K.; Armstrong, W. H. *J. Am. Chem. Soc.* **1991**, *113*, 5055 and references therein.
(22) Suzuki, M.; Hayashi, Y.; Munezawa, K.; Suenaga, M.; Senda, H.; Uehara, A. *Chem. Lett.* **1991**, 1929.
(23) Mikuriya, M.; Yamato, Y.; Tokii, T. *Chem. Lett.* **1991**, 1429.
(24) Ashmawy, F. M.; McAuliffe, C. A.; Parish, R. V.; Tames, J. *J. Chem. Soc., Chem. Commun.* **1984**, 14.
(25) (a) Kambara, T.; Govindjee. *Proc. Natl. Acad. Sci. U.S.A.* **1985**, *82*, 6119. (b) Renger, G. *Chem. Scr.* **1988**, *28A*, 105. (c) Proserpio, D. M.; Hoffmann, R.; Dismukes, G. C. *J. Am. Chem. Soc.* **1992**, *114*, 4347.
(26) (a) Velthuys, B.; Kok, B. *Biochim. Biophys. Acta* **1978**, *502*, 211. (b) Mano, J.; Takahashi, M.; Asaka, K. *Biochemistry* **1987**, *26*, 2495. (c) Frasch, W. D.; Mei, R. *Biochim. Biophys. Acta* **1987**, *891*, 8.

0020-1669/92/1331-4987$03.00/0

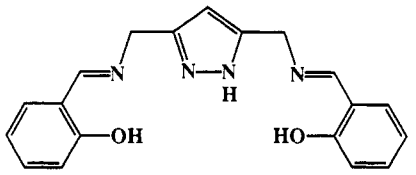

Figure 1. Chemical structure of H_3L.

Table I. Crystal Data for $[Mn_4(L)_2(CH_3O)_4(CH_3OH)_4](ClO_4)_2 \cdot 4CH_3OH$

formula	$C_{50}H_{74}Cl_2Mn_4N_8O_{24}$	β/deg	103.98 (5)
color of cryst	brown	γ/deg	92.77 (6)
fw	1461.83	V/Å^3	1611 (1)
cryst dimens/mm^3	0.40 × 0.38 × 0.33	Z	1
cryst syst	triclinic	D_c/g cm^{-3}	1.503
space group	$P\bar{1}$	D_m/g cm^{-3}	1.502
a/Å	13.663 (6)	μ(Mo Kα)/cm^{-1}	8.98
b/Å	14.536 (4)	no. of reflcns	4525
c/Å	8.483 (4)	R^a/%	7.68
α/deg	98.59 (4)	$R_w^{b,c}$/%	7.34

^{a} $R = \sum||F_o| - |F_c||/\sum|F_o|$. ^{b} $R_w = \{\sum[w(|F_o| - |F_c|)^2]/\sum[w|F_o|^2]\}^{1/2}$. ^{c} $w = 1/\sigma|F_o|$.

exhibits catalase-like activity in the dark when hydrogen peroxide is added as the substrate.[26] This fact suggests similar active site structures of Mn catalase and the OEC of PSII despite their different nuclearity. In view of the above facts, the design of new dinuclear and tetranuclear manganese complexes that bear a site for binding H_2O_2 is very important to provide insight into the mechanistic function of both Mn catalase and the OEC of PSII.

In this study we have prepared 3,5-bis((salicylideneamino)-methyl)pyrazole (Figure 1; abbreviated as H_3L) with the hope of providing new dinuclear manganese complexes. The bridging function of the pyrazolate ion is well-known,[27,28] and dinucleating ligands containing a pyrazolate group as the endogenous bridge have been developed in our laboratory.[28,29] H_3L is such a ligand that may incorporate a pair of manganese ions with its two tridentate coordination sites with the NNO donor set, i.e. pyrazolate N and salicylideneaminate N and O. The bridge by the endogenous pyrazolate group provides the Mn- -Mn separation of 3.4–3.7 Å, and the fourth equatorial sites of the bound manganese ions can be available for a bridge with peroxide ion as the substrate. A manganese complex of the formula $Mn_2(L)(OCH_3)_2(CH_3OH)_4(ClO_4)$ has been obtained whose crystal structure and some physicochemical properties are reported.

Experimental Section

Measurements. Elemental analyses of carbon, hydrogen, and nitrogen were obtained at the Elemental Analysis Service Center of Kyushu University. Analyses of Mn were made on a Shimadzu AA-660 atomic absorption/flame emission spectrophotometer. Infrared (IR) spectra were recorded on a JASCO IR-810 spectrometer on KBr disks or Nujol mulls. Electronic absorption spectra were measured in *N,N*-dimethylformamide (DMF) and on powder samples with a Shimadzu UV-210 spectrophotometer. H-NMR spectra (400 MHz) were recorded on a JEOL JNM-GX 400 spectrometer in methanol-d_4 using tetramethylsilane as the internal standard. Solid-state magnetic susceptibility measurements were made on a Hoxan HSM-D SQUID magnetometer in the temperature range 4.2–100 K and on a Faraday balance in the range 80–300 K.

Preparation of 3,5-Bis((salicylideneamino)methyl)pyrazole (H_3L). 3,5-Bis(aminomethyl)pyrazole dihydrochloride[29] (500 mg, 2.5 × 10^{-3} mol) was dissolved in water (15 cm^3), and the solution was neutralized with LiOH·H_2O (210 mg, 5 × 10^{-3} mol) dissolved in a minimum amount of water. To this was added a methanolic solution (10 cm^3) of salicylaldehyde (620 mg, 5 × 10^{-3} mol) with stirring to result in the precipitation of yellow microcrystals. They were recrystallized from methanol in a yield of 600 mg (70%). Mp: 154–156 °C. Anal. Calcd for $C_{19}H_{18}N_4O_2$: C, 68.25; H, 5.43; N, 16.76. Found: C, 68.10; H, 5.40; N, 16.63. H-NMR (CD_3OD, δ/ppm): 8.52 (s, 2H), 7.37 (m, 4H), 6.90 (m, 4H), 6.23 (s, 1H), 4.77 (s, 4H). IR bands (cm^{-1}): 3180–2480 (multi, m), 1950 (w), 1638 (vs), 1610 (m), 1580 (m), 1533 (s), 1490 (s), 1278 (s), 1218 (s), 1145 (s), 758 (s). UV–vis data [λ/nm (ϵ/M^{-1} cm^{-1})] in DMF: 270 (38 000), 320 (24 000), 400 (sh, 90).

Preparation of $Mn_4(L)_2(CH_3O)_4(CH_3OH)_8(ClO_4)_2$. To a solution of H_3L (35 mg, 1 × 10^{-4} mol) in dry methanol (15 cm^3) were added manganese(II) acetate tetrahydrate (50 mg, 2 × 10^{-4} mol) and sodium perchlorate (25 mg, 2 × 10^{-4} mol), and the mixture was stirred at ambient temperature to form a clear brown solution. The solution was neutralized to pH 7 with triethylamine, filtered to separate any insoluble materials, and allowed to stand in a refrigerator to form efflorescent brown needles. The yield was 32 mg (50%). Anal. Calcd for $C_{42}H_{50}Cl_2Mn_4N_8O_{20}$: C, 39.49; H, 3.94; N, 8.77; Mn, 17.2. Found: C, 39.54; H, 3.61; N, 8.95; Mn, 16.5. IR bands (cm^{-1}): 3400 (br, s), 2925 (w), 2808 (w), 1620 (vs), 1541 (s), 1444 (m), 1297 (s), 1286 (s), 1147 (s), 1118 (s), 1082 (s), 1042 (m), 903 (m), 827 (m), 758 (m), 622 (s). UV–vis data [λ/nm (ϵ/M^{-1} cm^{-1})]: in DMF, 270 (56 000), 390 (13 000), 580 (380); as a solid, 280, 390, 500, 580.

X-ray Structure Analysis. A crystal of approximate dimensions of 0.40 × 0.38 × 0.33 mm^3 was used for the structure analysis. Intensities and lattice parameters were obtained on a Rigaku Denki AFC-5 automated four-circle diffractometer with graphite-monchromated Mo Kα radiation

Table II. Final Atomic Coordinates for Non-Hydrogen Atoms (×10^4) of $[Mn_4(L)_2(CH_3O)_4(CH_3OH)_4](ClO_4)_2 \cdot 4CH_3OH$

atom	x	y	z	B_{eqv}/Å^2
Mn1	3587 (1)	2570 (1)	2518 (2)	3.4
Mn2	5041 (1)	1071 (1)	641 (1)	2.9
O1	3969 (4)	3557 (4)	4270 (7)	4.1
O2	4816 (4)	−2113 (3)	434 (6)	3.7
N1	2159 (5)	2904 (4)	1924 (8)	4.0
N2	3017 (5)	1642 (4)	553 (7)	3.4
N3	3476 (4)	983 (4)	−220 (7)	3.1
N4	3412 (5)	−1099 (4)	−1493 (7)	3.2
C1	3944 (7)	4958 (5)	6008 (10)	4.2
C2	3437 (8)	5679 (6)	6527 (11)	5.3
C3	2431 (8)	5733 (6)	5830 (12)	6.0
C4	1922 (7)	5050 (7)	4557 (13)	5.9
C5	2423 (6)	4301 (6)	3977 (10)	4.3
C6	3445 (6)	4251 (5)	4720 (10)	3.8
C7	1824 (6)	3611 (6)	2647 (11)	4.5
C8	1417 (6)	2245 (6)	588 (12)	5.1
C9	2014 (6)	1540 (6)	−158 (10)	3.8
C10	1791 (6)	775 (5)	−1427 (9)	3.7
C11	2738 (6)	444 (5)	−1402 (9)	3.1
C12	2950 (6)	−393 (5)	−2503 (9)	3.3
C13	2766 (6)	−1651 (5)	−1128 (10)	3.8
C14	3004 (6)	−2350 (5)	−64 (10)	3.8
C15	2172 (7)	−2840 (6)	271 (12)	5.5
C16	2344 (8)	−3492 (7)	1314 (12)	6.0
C17	3320 (7)	−3689 (6)	1997 (11)	5.2
C18	4141 (7)	−3234 (6)	1696 (10)	4.2
C19	3994 (6)	−2551 (5)	646 (9)	3.4
CL	145 (2)	−2095 (2)	5461 (4)	8.3
O3	1037 (8)	−2254 (7)	5103 (15)	14.3
O4	153 (10)	−1174 (7)	5923 (22)	23.2
O5	−682 (10)	−2371 (9)	4346 (19)	24.3
O6	190 (11)	−2492 (14)	6675 (18)	27.0
OM1	4834 (4)	2040 (3)	2717 (6)	3.4
CM1	5565 (6)	2168 (6)	4245 (10)	4.3
OM2	4921 (4)	−40 (3)	1483 (6)	3.0
CM2	4333 (7)	−176 (6)	2612 (10)	4.4
OM3	3098 (5)	1635 (4)	4195 (7)	5.3
CM3	3146 (9)	1960 (7)	5903 (11)	6.9
OM4	4094 (5)	3487 (4)	786 (7)	5.2
CM4	3452 (9)	3958 (8)	−385 (13)	7.6
OM5	1498 (7)	346 (6)	3198 (13)	12.4
CM5	1297 (10)	−519 (8)	2262 (17)	9.9
OM6	255 (10)	4074 (10)	8482 (18)	20.3
CM6	802 (13)	4636 (12)	8026 (23)	16.0

(27) (a) Trofimenko, S. *Chem. Rev.* **1972**, *72*, 497. (b) Inoue, M.; Kubo, K. *Coord. Chem. Rev.* **1976**, *21*, 1. (c) Ajo, D.; Bencini, A.; Mani, F. *Inorg. Chem.* **1988**, *27*, 2437.
(28) Kamiusuki, T.; Ōkawa, H.; Inoue, K.; Matsumoto, N.; Kodera, M.; Kida, S. *J. Coord. Chem.* **1991**, *23*, 201 and references therein.
(29) (a) Kamiusuki, T.; Ōkawa, H.; Kitaura, E.; Koikawa, M.; Matsumoto, N.; Kida, S.; Oshio, H. *J. Chem. Soc., Dalton Trans.* **1989**, 2077. (b) Kamiusuki, T.; Ōkawa, H.; Matsumoto, N.; Kida, S. *Ibid.* **1990**, 195. (c) Kamiusuki, T.; Ōkawa, H.; Kitaura, E.; Inoue, K.; Kida, S. *Inorg. Chim. Acta* **1991**, 179, 139.

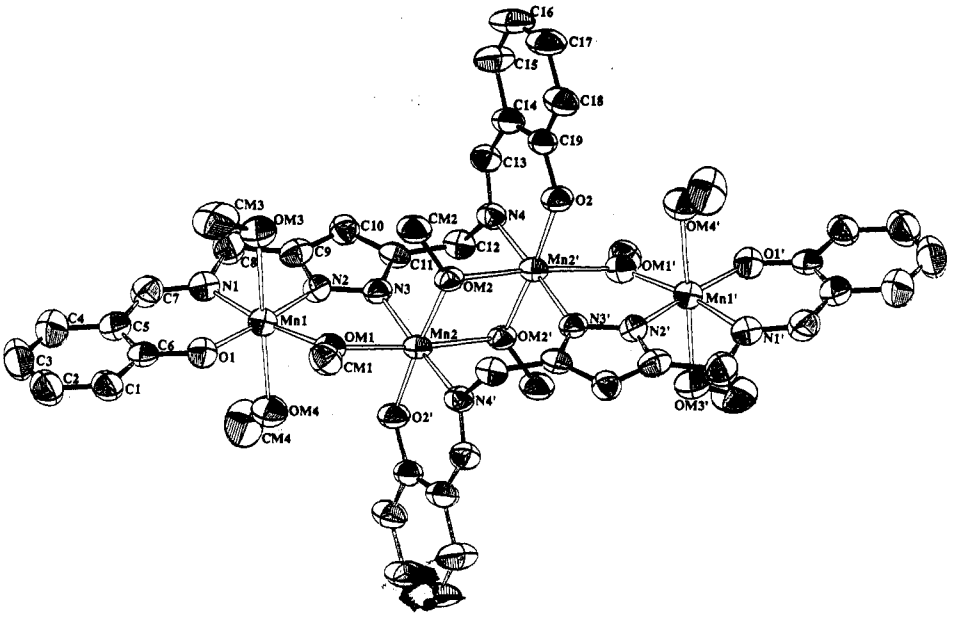

Figure 2. ORTEP view of the tetranuclear complex cation with the numbering scheme.

($\lambda = 0.710\,69$ Å) at 20 ± 1 °C. Three standard reflections were monitored every 150 reflections and showed no systematic decrease in the intensity. For the intensity data collection the ω–2θ scan mode was used at a scan rate of 4° min^{-1} in the range $2.5° \leq 2\theta \leq 52°$. The scan width was $(1.00 + 0.35 \tan\theta)°$. The octant measured was $+h,k,l$. A total of independent reflections with $|F_o| > 3\sigma(|F_o|)$ were used for the analysis. A summary of data collection and crystal data is given in Table I.

The structure was solved by the standard heavy-atom method and refined by the block-diagonal least-squares method, where the function minimized is $\sum w(|F_o| - |F_c|)^2$ and weight $w = 1/\sigma(|F|)$ was adopted for all reflections. The contributions for hydrogen atoms bound to carbons were introduced in the calculated positions. These hydrogen atoms were included in the structure factor calculation but were not refined. The atomic scattering factors were taken from ref 30. Absorption corrections were not applied. All computations were carried out on a FACOM M 780 computer at the Computer Center of Kyushu University using the UNICS III program system.[31] The final atomic coordinates are given in Table II.

Results and Discussion

The crystal of the complex consists of the centrosymmetric complex cation $[Mn_4L_2(CH_3O)_4(CH_3OH)_4]^{2+}$, two perchlorate ions, and four methanol molecules captured in the crystal lattice. The ORTEP view of the cation is shown in Figure 2, together with the numbering scheme. Selected bond distances and angles are given in Table III.

The crystal structure analysis has revealed the dimerized tetranuclear structure with a linear array of four manganese ions for the complex cation. In the cation are involved two ligands in the deprotonated form (L^{3-}), four bridging methoxide ions, and four methanol molecules. This leads to our conclusion that all the manganese ions are in the same 3+ oxidation state. Each terminal Mn(III) ion (Mn1) is bound to one NNO-coordination site of L^{3-}, through the pyrazolate nitrogen N2 and salicylideneaminate nitrogen N1 and oxygen O1, and has a six-coordinate environment together with two methanol oxygens OM3 and OM4 and one methoxide oxygen OM1 acting as the bridge to the adjacent internal Mn(III) ion, Mn2. The Mn1–OM3 and Mn1–OM4 bond distances (2.295 (7) and 2.324 (7) Å, respectively) are elongated relative to the other four bond distances (1.885 (5)–1.995 (7) Å). This may be due to the Jahn–Teller distortion for high-spin Mn(III) ion. The pyrazolate nitrogen N3 of the other NNO site of the ligand coordinates to the adjacent internal Mn ion, Mn2, but the salicylideneaminate N4 and O2 are associated with coordination to another internal Mn(III) ion, Mn2′. In the same way N3′ coordinates to Mn2′ while N4′ and O2′ coordinate to Mn2, affording the linear array of Mn1- -Mn2- -Mn2′- -Mn1′. Two internal Mn(III) ions, Mn2 and Mn2′, are bridged to each other by two methoxide oxygens OM2 and OM2′. The geometry about Mn2 is also six-coordinate with pyrazolate N3, salicylideneaminate N4′ and O2′, and bridging methoxide oxygens OM1, OM2, and OM2′. The Jahn–Teller distortion is seen along the OM1–Mn2–OM2′ axis. The Mn1- -Mn2 separation bridged by the pyrazolate and methoxide groups is 3.485 (3) Å. The Mn2- -Mn2′ separation bridged by two methoxide groups is 3.127 (2) Å.

Table III. Selected Bond Distances (Å) and Angles (deg) for $[Mn_4(L)_2(CH_3O)_4(CH_3OH)_4](ClO_4)_2 \cdot 4CH_3OH$

Bond Distances					
Mn1–Mn2	3.485 (3)	Mn2–Mn2′	3.127 (2)		
Mn1–O1	1.859 (5)	Mn1–N1	1.996 (7)	Mn1–N2	1.951 (6)
Mn1–OM1	1.885 (5)	Mn1–OM3	2.295 (7)	Mn1–OM4	2.324 (7)
Mn2–N3	2.077 (6)	Mn2–OM1	2.169 (5)	Mn2–OM2	1.876 (5)
Mn2–O2′	1.906 (6)	Mn2–N4′	2.058 (6)	Mn2–OM2′	2.177 (5)

Bond Angles			
Mn1–OM1–Mn2	118.4 (2)	Mn2–OM2–Mn2′	100.7 (2)
O1–Mn1–N1	92.9 (3)	O1–Mn1–OM1	99.2 (2)
O1–Mn1–OM3	90.6 (2)	O1–Mn1–OM4	90.5 (2)
N1–Mn1–N2	79.2 (3)	N1–Mn1–OM3	87.5 (3)
N1–Mn1–OM4	93.2 (3)	N2–Mn1–OM1	88.8 (2)
N2–Mn1–OM3	92.1 (3)	N2–Mn1–OM4	86.9 (3)
OM1–Mn1–OM3	91.6 (2)	OM1–Mn1–OM4	87.4 (2)
N3–Mn2–OM1	85.8 (2)	N3–Mn2–OM2	89.4 (2)
N3–Mn2–O2′	91.1 (2)	N3–Mn2–OM2′	88.5 (2)
OM1–Mn2–OM2	98.3 (2)	OM1–Mn2–O2′	88.2 (2)
OM1–Mn2–N4′	95.4 (2)	OM2–Mn2–N4′	88.5 (2)
OM2–Mn2–OM2′	79.3 (2)	O2′–Mn2–N4′	90.9 (2)
O2′–Mn2–OM2′	94.2 (2)	N4′–Mn2–OM2′	90.2 (2)

The solid-state magnetic susceptibility of the complex was measured in the temperature range 4.2–300 K. The temperature dependence of the magnetic moment μ_{eff} per Mn atom is given in Figure 3. The magnetic moment at room temperature is 4.92 μ_B, which is common for high-spin Mn(III) ($S = 2$). The moment decreases with lowering of temperature, very gradually in the high-temperature region but more abruptly at low temperature, down to 2.91 μ_B at 4.2 K.

The derivation of the magnetic susceptiblity expression for the linear Mn(III)–Mn(III)–Mn(III)–Mn(III) system is not easy

(30) *International Tables for X-Ray Crystallography*; Ibers, J. A., Hamilton, W. C., Eds.; Knoch Press: Birmingham, U.K., 1974; Vol. 4.
(31) Sakurai, T.; Kobayashi, K. *Rikagaku Kenkyusho Hokoku* **1979**, *55*, 69.

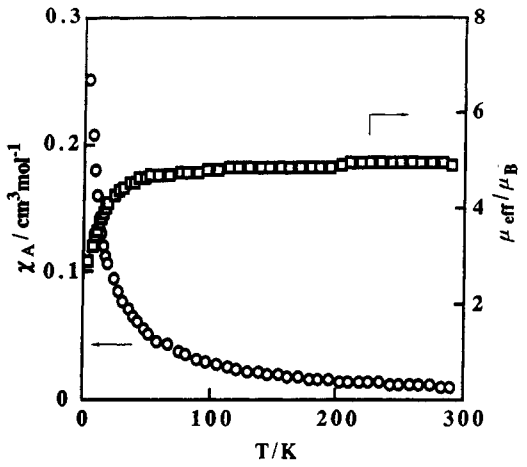

Figure 3. Temperature dependence of effective magnetic moment (□) and magnetic susceptibility (○) per Mn atom.

because Kambe's approach[32] cannot be applied for such linear tetranuclear cases. The susceptibility expression may be obtained on the basis of the spin Hamiltonian $\mathcal{H} = -2J(S_1S_2 + S_3S_4) - 2J'S_2S_3$ with $J_{12} = J_{34} = J$ and $J_{23} = J'$ for Mn^1–Mn^2–Mn^3–Mn^4 and using 625 possible wave functions $\phi_k = |m_{s1},m_{s2},m_{s3},m_{s4}\rangle$,[33,34] but this general treatment of exchange interaction necessitates laborious tasks to determine the matrix elements $\langle\phi_k|\mathcal{H}|\phi_l\rangle$ for all the wave functions, to diagonalize the resulting 625 × 625 matrix, etc. Because of this difficulty, detailed magnetic analyses were not done for the Mn complex, but Figure 3 clearly indicates that all the manganese ions in the complex are in a 3+ oxidation state and the overall magnetic behavior is weakly antiferromagnetic. The EPR spectra of the complex, measured on solid samples and in DMF solutions at room temperature and liquid-nitrogen temperature, were not definitive, probably because of the antiferromagnetic spin-exchange interaction.

The solid-state electronic spectrum of the complex shows two intense bands at 280 and 390 nm and two weak bands at 500 and 580 nm. The absorptions at 280 and 390 nm are assigned to the π–π^* transitions of the aromatic ring and the C=N linkage, respectively.[35,36] Two weak bands in the visible region are assigned to the d–d transition bands of Mn(III) ions.[23,37]

The absorption spectrum of the complex in DMF resembles the reflectance spectrum in the region 250–700 nm, but the visible absorption at 500 nm is lacking. This fact implies that the complex structure in DMF differs from the tetranuclear structure in the solid state. We have found that the complex shows a high catalytic activity to disproportionate hydrogen peroxide in DMF. Details of the catalase-like activity will be reported together with results on other manganese complexes of related pyrazole-containing dinucleating ligands.

Acknowledgment. The authors thank Mr. Msaaki Ohba and Mr. Minoru Mitsumi for their help in the magnetic susceptibility measurements. This work was supported by a Grant-in-aid for Scientific Research on Priority Area (No. 03241105).

Supplementary Material Available: Listings of atomic positional and anisotropic thermal parameters (Table 2) and complete bond lengths and angles with their estimated standard deviations (Table 3) (5 pages). Ordering information is given on any current masthead page.

(32) Kambe, K. *J. Phys. Soc. Jpn.* **1950**, *5*, 48.
(33) Sinn, E. *Coord. Chem. Rev.* **1970**, *5*, 313.
(34) Mabbs, F. E.; Machin, D. J. *Magnetism and Transition Metal Complexes*; Chapman and Hall: London, 1973.
(35) Bosnich, B. *J. Am. Chem. Soc.* **1968**, *90*, 627.
(36) Downing, R. S.; Urbach, F. L. *J. Am. Chem. Soc.* **1969**, *91*, 5977.
(37) (a) Dey, K.; Ray, K. C. *J. Inorg. Nucl. Chem.* **1975**, *37*, 695. (b) Boucher, L. J.; Coe, C. G. *Inorg. Chem.* **1976**, *15*, 1334. (c) Torihara, N.; Mikuriya, M.; Ōkawa, H.; Kida, S. *Bull. Chem. Soc. Jpn.* **1980**, *53*, 1610. (d) Bertoncello, K.; Fallon, G. D.; Murray, K. S.; Tiekink, E. R. T. *Inorg. Chem.* **1990**, *30*, 3562.